Available online at www.sciencedirect.com
ScienceDirect
Applied Geochemistry 22 (2007) 1841–1859
Applied Geochemistry
www.elsevier.com/locate/apgeochem

Accelerated weathering of high-level and plutonium-bearing lanthanide borosilicate waste glasses under hydraulically unsaturated conditions

Eric M. Pierce [a,*], B.P. McGrail [a], P.F. Martin [a], J. Marra [b], B.W. Arey [a], K.N. Geiszler [a]

[a] *Environmental Technology Directorate, Pacific Northwest National Laboratory, P.O. Box 999, MS: K6-81, Richland, WA 99352, United States*
[b] *Savannah River National Laboratory, Westinghouse Savannah River Company, Aiken, SC 29808, United States*

Received 15 December 2005; accepted 8 March 2007
Editorial handling by M. Gascoyne
Available online 10 May 2007

Abstract

The US Department of Energy (DOE) has proposed that a can-in-canister waste package design be used for disposal of excess weapons-grade Pu at the proposed mined geologic repository at Yucca Mountain, Nevada. This configuration consists of a high-level waste (HLW) canister fitted with a rack that holds mini-canisters containing a Pu-bearing lanthanide borosilicate (LaBS) waste glass and/or titanate-based ceramic (~15% of the total canister volume). The remaining volume of the HLW canister is then filled with HLW glass (~85% of the total canister volume). A 6-a pressurized unsaturated flow (PUF) test was conducted to investigate waste form–waste form interactions that may occur when water penetrates the canisters and contacts the waste forms. The PUF column volumetric water content was observed to increase steadily during the test because of water accumulation associated with alteration phases formed on the surfaces of the glasses. Periodic excursions in effluent pH, electrical conductivity, and solution chemistry were monitored and correlated with the formation of a clay phase(s) during the test. Geochemical modeling, with the EQ3NR code, of select effluent solution samples suggests the dominant secondary reaction product for the surrogate HLW glass, SRL-202, is a smectite di-octahedral clay phase(s), possibly nontronite [$Na_{0.33}$ $Fe_2(AlSi)_4O_{10}(OH)_2 \cdot n(H_2O)$] or beidellite [$Na_{0.33}Al_{2.33}Si_{3.67}O_{10}(OH)_2$]. This clay phase was identified in scanning electron microscope (SEM) images as discrete spherical particles growing out of a hydrated gel layer on reacted SRL-202 glass. Alpha energy analysis (AEA) of aliquots of select effluent samples that were filtered through a 1.8 nm filter suggest that approximately 80% of the total measurable Pu was in the form of a filterable particulate, in comparison to unfiltered aliquots of the same sample. These results suggest the filterable particles are >1.8 nm but smaller than the 0.2 μm average diameter openings of the Ti porous plate situated at the base of the column. In this advection-dominated system, Pu appeared to be migrating principally as or in association with colloids after being released from the LaBS glass. Analyses of reacted LaBS glass particles with SEM with energy dispersive X-ray spectroscopy suggest that Pu may have segregated into a discrete disk-like phase, possibly PuO_2. Alteration products that contain the neutron absorber Gd have not been positively identified. Separation of the Pu and the neutron absorber Gd during

* Corresponding author.
E-mail address: Eric.Pierce@pnl.gov (E.M. Pierce).

0883-2927/$ - see front matter
doi:10.1016/j.apgeochem.2007.03.056

glass dissolution and transport could be a criticality issue for the proposed repository. However, the translation and interpretation of these long-term PUF test results to actual disposed waste packages requires further analysis.

1. Introduction

Representatives of Russia and the United States held discussions in the 1990s about the disposition of approximately 50 metric tons (MT) of surplus weapons-grade Pu (Rankin and Gould, 2000). During these discussions, a preliminary environmental impact statement was completed. In response to the results presented in the preliminary environmental impact statement, the US Department of Energy (DOE) implemented a program to provide for the safe and secure storage of surplus weapons-grade Pu. As part of this program, DOE decided to build (1) the Pit Disassembly and Conversion Facility (PDCF), (2) the Mixed Oxide Fuel Fabrication Facility (MFFF), and (3) the Plutonium Immobilization Plant (PIP) at the Savannah River Site in west-central South Carolina (Rankin and Gould, 2000). DOE also decided that the can-in-canister design was the preferred option for the disposal of an immobilized Pu-bearing waste form at the proposed mined geologic repository at Yucca Mountain, Nevada (Rankin and Gould, 2000). This configuration consists of a high-level waste (HLW) canister (approximately 0.6 m outer diameter and 3 m tall) fitted with a rack that holds mini-canisters (approximately 0.1 m outer diameter and 0.5 m tall) containing a Pu-bearing ceramic and/or glass (~15% of the total canister volume). The remaining volume of the HLW canister is then filled with HLW glass (~85% of the total canister volume). The use of this can-in-canister design provides secure storage for Pu, because the engineered barrier created by the HLW glass requires a heavily shield facility to retrieve the Pu which makes retrieval difficult.

Although a titanate-based ceramic was previously selected as the Pu-immobilization waste form (Cochran et al., 1997; Gray et al., 1997; Myers et al., 1997), the use of glass, namely a lanthanide borosilicate (LaBS), instead of ceramic has reemerged as a candidate waste form (Marra and Ebert, 2003). This occurred because, unlike the titanate-based ceramic, glass can accommodate the wide variety of impurities that is associated with highly impure weapons-grade Pu currently slated for disposition. Before DOE can conduct a credible safety analysis, information on long-term dissolution of these waste glasses in a can-in-canister configuration must be evaluated.

The long-term dissolution of nuclear waste glasses, including HLW, low-activity waste (LAW), and Pu-bearing LaBS and Alkali-Tin-Silicates (ATS) glasses, has been studied for more than two decades (Bates et al., 1982, 1995, 1996; Bibler et al., 1996; Ebert and Bates, 1993; Ebert and Tam, 1997; Gin et al., 2001; McGrail et al., 2001; Ramsey et al., 1995; Vernaz et al., 2001). Although these results are useful, some of the test methods used for these studies yielded data with limited applicability to the development of models that describe the long-term behavior of glass under repository-relevant conditions. The majority of the available results on the accelerated weathering of these waste forms have been produced with static test methods, such as the vapor hydration test (VHT) (Bates et al., 1982) and product consistency test (PCT) (ASTM, 1994; Jantzen and Bibler, 1987). Both VHT and PCT are closed-system tests conducted under conditions that are quite different from the open-system conditions expected in a geologic repository. Specifically, VHT and PCT do not allow for mass transport processes to occur, such as the transport of water and/or atmospheric gases. The VHT is an unsaturated test method for which a specimen is suspended in a container with a specified volume of water required to obtain a target water vapor saturation. This test method provides critical information about the secondary phase paragenesis of the waste form, but no information is obtained about the solution chemistry in contact with the glass, which is required for long-term performance assessment. Contrary to VHT, PCT is a water-saturated static test. For a PCT, dissolved material is allowed to accumulate in the aqueous phase, thus altering the chemistry of the solution in contact with the glass. Although information about the solution chemistry is obtained, these changes may not be representative of the solution chemistry that is expected in an open-system disposal facility. For a more detailed discussion on the dissolution of HLW glasses see Bates et al.

(1994a,b) and of LAW glasses see McGrail et al. (2001) and Pierce et al. (2004) as well as the references contained therein.

A lanthanide borosilicate glass, based upon a commercial glass formulation created in the 1930s (Loffler, 1932), was developed at the Savannah River Site as a high-temperature glass composition that can be used to incorporate Pu (Plodinec, 1979; Ramsey et al., 1995). Unlike typical HLW and LAW glasses that contain as much as 20 mass% Na_2O, LaBS glass is devoid of alkalis. This lack of alkalis is believed to be the cause of the decreased dissolution rate observed in PCTs conducted with LaBS, approximately 20–50 times lower than rates measured in PCTs conducted with typical HLW glass (Mertz et al., 1998). Although a few researchers have examined the dissolution of LaBS glass with the VHT, PCT, and SPFT methods (Bates et al., 1995; Bibler et al., 1996; Fortner et al., 2000; Mertz et al., 1998; Ramsey et al., 1995; Strachan et al., 1998), none of these studies addressed the long-term dissolution in a can-in-canister waste package configuration under repository-relevant conditions.

In the can-in-canister configuration, several scenarios of water contact are possible. From a hydrodynamic viewpoint, after water has breached the container, the most credible contact mode is the slow percolation of water through the waste package under conditions of partial hydraulic saturation. Under these open-flow and transport conditions, water flow through the container is expected to be controlled by gravity and capillary forces. The greater proportion of HLW glass in comparison to LaBS glass suggests that, on average, the dissolution of the HLW glass will dominate the solution chemistry of any water percolating through a can-in-canister waste package. The objectives for this investigation were to (1) understand how the HLW glass-water interaction impacts the release and transport of Pu, (2) evaluate the paragenesis of secondary phases, and (3) evaluate the release of neutron absorbers. In addition to the above objectives, the main objective for this study was to accurately assess the dissolution of HLW and LaBS glass in this can-in-canister configuration with an unsaturated flow-through test method in which repository conditions are closely mimicked. As a result of the above objectives, the canister metals were not included in this test and should be considered for future experiments. In this paper, the results from a 6-a waste form-waste form interaction experiment conducted in a sandwich configuration (i.e., representative of the can-in-canister configuration) with the PUF test method are we summarized. The term waste form-waste form, in this document refers to the relationship between the two glasses used in the experiment, LaBS glass and a simulated HLW borosilicate glass, SRL-202.

2. Glass chemistry and material preparation

The SRL-202 glass and LaBS frit (without PuO_2) were prepared by mixing measured amounts of dried reagent-grade chemicals in a ceramic ball mill. The mixtures were melted at 1450 °C for 1 h in a Pt (90%) Rh (10%) crucible, and the molten glass was poured onto a cool stainless steel plate. After being quenched, the LaBS frit was ground into a powder with a ceramic ball mill and mixed with PuO_2 in a ratio of 4.5 g of PuO_2 to 35.5 g of LaBS frit. The LaBS frit and PuO_2 mixture was then melted at

Table 1
Chemical composition (mass%), particle density, geometric and BET surface area, and surface roughness for SRL-202 and LaBS glasses

Oxide	SRL-202	LaBS
Al_2O_3	4.8	19.0
B_2O_3	7.0	10.4
CaO	1.1	n.d.
Fe_2O_3	12.6	n.d.
Gd_2O_3	n.d.	7.6
K_2O	2.0	n.d.
La_2O_3	n.d.	11.0
Li_2O	4.5	n.d.
MgO	1.5	n.d.
MnO	3.3	n.d.
Na_2O	7.9	n.d.
Nd_2O_3	0.4	11.4
NiO	1.1	n.d.
PuO_2	n.d.	11.4
SiO_2	51.5	25.8
SrO	n.d.	2.2
ZrO_2	1.2	1.2
Others[a]	1.2	n.d.
Total	100.0	100.0
F.W.	65.98	107.88
ρ	$(2.71 \pm 0.01) \times 10^3$	$(3.56 \pm 0.01) \times 10^3$
S_{geo}	4.2 ± 0.8	3.2 ± 0.6
S_{BET}	19.0 ± 0.2	n.d.
S.R.	4.5	n.d.

n.d. – not determined, F.W. – formula weight (g/mol), ρ – particle density (kg/m^3), S_{geo} – geometric surface area (m^2/kg), S_{BET} – Kr-adsorption BET surface area (m^2/kg), S.R. – surface roughness factor (ratio of S_{BET} to S_{geo}) (unitless).

[a] Others include $Cr_2O_3 = 0.33\%$, $CuO = 0.36\%$, $PbO = 0.16\%$, $TiO_2 = 0.24\%$, and $ZnO = 0.09\%$.

1450 °C and periodically stirred to produce 40.0 g of Pu-bearing LaBS glass. For the remainder of this document the Pu-bearing LaBS glass will be referred to as LaBS. The composition of each glass (see Table 1) was confirmed by use of inductively coupled plasma optical emission spectroscopy (ICP-OES) and mass spectrometry (ICP-MS) analyses of Na_2O_2 and $LiBO_2$ fusions of glass samples.

The SRL-202 glass specimen contains 19 components with the concentration of Al_2O_3, B_2O_3, CaO, Fe_2O_3, K_2O, Li_2O, MgO, MnO, Na_2O and SiO_2 comprising of 96.2 mass% of the glass with minor amounts of other oxides such as Cr_2O_3, CuO, Nd_2O_3, NiO, PbO, TiO_2, ZnO and ZrO_2. Unlike the SRL-202 glass specimen, the LaBS glass specimen is devoid of alkalis (Na_2O, K_2O, and Li_2O) and contains as much as 11.4 mass% PuO_2. Approximately 30 mass% of the LaBS glass is composed of rare earths (Gd_2O_3, La_2O_3, Nd_2O_3) with the remaining amount consisting of Al_2O_3, B_2O_3, PuO_2, SiO_2, SrO and ZrO_2. The rare earth Gd, 7.6 mass% Gd_2O_3, was added to the LaBS as a neutron absorber.

The SRL-202 and LaBS glass specimens used in these experiments were prepared by crushing the samples in a ceramic ball mill. The crushed glass was then sieved into the desired size fraction, <250 to >170 μm (<20 to >70 mesh), with ASTM standard sieves (ASTM, 2001). After being sized, the glass specimens were washed in 18 MΩ ultra pure deionized water (DIW), washed again with 18 MΩ DIW in an ultrasonic bath, rinsed in ethanol, and dried in an oven at 90 °C (±2 °C). Each glass sample, before and after testing, was stored at room temperature (~23 °C) in a seal container dessicator that contained $CaSO_4$.

2.1. Specific surface area measurement and calculation

The specific surface area of each specimen was calculated with a geometric formula (McGrail et al., 1997b) Eq. (1),

$$S_{geo} = \frac{3}{\rho r} \quad (1)$$

where S_{geo} is the surface area (m^2/kg), ρ is the glass density (kg/m^3), and r is average radius (m). The glass density, measured with a He gas pycnometer (Micromeritics, Norcross, Georgia), was determined to be 2.71×10^3 kg/m^3 for SRL-202 glass and 3.56×10^3 kg/m^3 for LaBS glass, with a corresponding geometric surface area of 4.2 ± 0.8 m^2/kg (i.e., 0.0042 ± 0.0008 m^2/g) and 3.2 ± 0.6 m^2/kg (i.e., 0.0032 ± 0.0006 m^2/g), respectively. Eq. (1) assumes the crushed particles are spherical with no surface flaws or porosity and the size distributions of the grains are normally distributed. For comparison, Kr-adsorption BET measurements were determined for the SRL-202 glass (Brunauer et al., 1938) and was determined to be 19.0 ± 0.2 m^2/kg (i.e., 0.019 ± 0.0002 m^2/g), which is approximately 4.5 times higher than the calculated geometric surface area. Because these glasses have very little, if any, porosity as confirmed by SEM, it is believed the higher value yielded by the Kr-BET analysis are the result of finer-grained particles (higher surface area particles) that have adhered to the material of the desired size fraction. The results are consistent with the results from experiments with low-activity waste glass monoliths (McGrail et al., 2000b), non-porous natural glasses (Wolff-Boenisch et al., 2004), as well as other borosilicate glasses (Papelis et al., 2003), which suggest the geometric surface area best represents the overall glass surface area. Therefore, the rates reported in this study were calculated with the geometric surface area. Another factor that complicates the estimate of specific surface area is the change each sample undergoes over the duration of the experiment. Therefore, the equation developed by McGrail et al. (1997b), which allows for the change in the sample mass over the duration of the experiment to be computed, was used to compensate for this effect. Changes in specimen masses were calculated from the background-corrected Li concentrations in the effluent solutions for SRL-202 and corresponded to a mass loss of ~12.4%; whereas the B_{LaBS} effluent concentration was used for LaBS glass and corresponded to a mass loss of ~2.7% after 6a of testing. The B_{LaBS} concentration was calculated by difference, additional details on extracting the B contribution from LaBS glass is discussed later in this paper.

3. Pressurized unsaturated flow (PUF) test method

The PUF apparatus (Fig. 1) allows for accelerated weathering experiments to be conducted under hydraulically unsaturated conditions, thereby mimicking the open-flow and transport properties of the disposal system environment while allowing the dissolving glass to achieve a final reaction state. The final reaction state, commonly referred to as stage III in the weathering process of glasses, is a

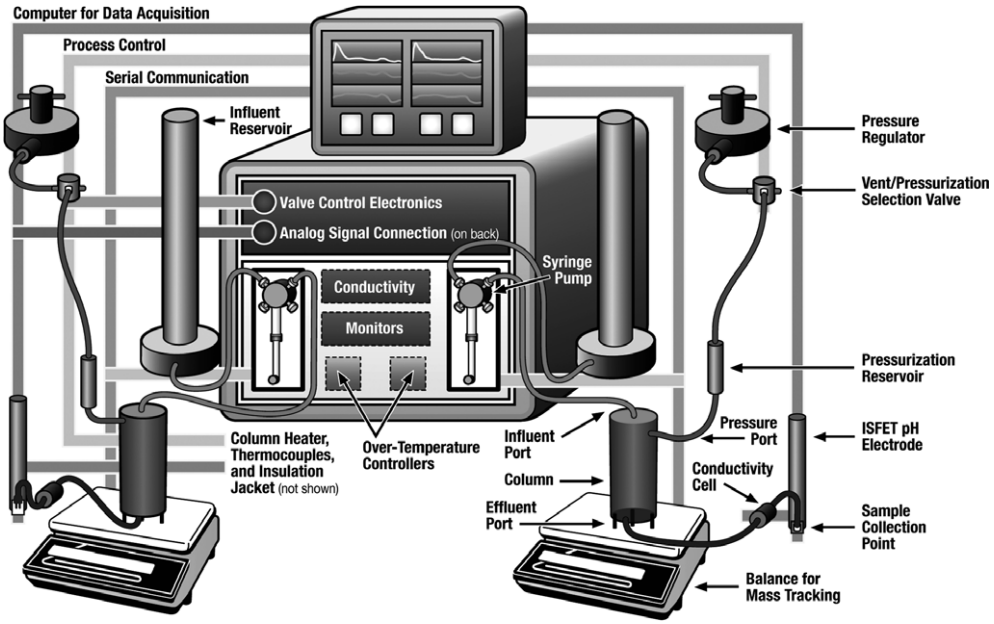

Fig. 1. Schematic of the second generation pressurized unsaturated flow (PUF) apparatus, which has the ability to conduct two simultaneous tests. The PUF apparatus consist of an influent reservoir, syringe pump, insulation wrapped column, electronic balance, pressure line and reservoir (PUF port), influent and effluent solution 1/16th Teflon lines, thermocouples (type J and type T), in line pH probe and electrical conductivity meter, collection vial, and a computer that records column weight, pH and electrical conductivity. The column was heated by applying an electrical current to a heat taped wrapped Al sleeve. A 0.2 μm Ti porous plate, situated at the base of the column, constant gas pressure, constant water flow, and gravity assisted drainage allows for the PUF column to operate under a hydraulically unsaturated condition.

point reached during long-term weathering that consists of the formation of secondary phases, while stage I and II mechanisms (e.g., network hydrolysis, ion exchange, and network dissolution) occur simultaneously. The PUF apparatus provides the capability to vary the volumetric water content from saturation to 20% or less, minimize the flow rate to increase liquid residence time, and operate at a maximum temperature of 90 °C. The PUF column operates under a hydraulically unsaturated condition by creating a steady-state vertical water flow, while maintaining uniform water content throughout the column; by using gravity to assist in drainage; and by maintaining a constant pressure throughout the column. Constant pressure is maintained with a porous Ti plate and gas pressure.

The PUF system and test procedure have been described previously by McGrail et al. (1996, 1999, 2000a) and Pierce et al. (2004, 2006), and only a general description is provided in this paper. The PUF system contains a 0.0762-m long and 0.0191-m diameter column fabricated from a chemically inert material, polyetheretherketone (PEEK), so that dissolution reactions are not influenced by interaction with the column material. A porous Ti plate with a nominal pore size of 0.2 μm is sealed in the bottom of the column to provide an adequate pressure differential for the conducting of fluid while operating under unsaturated conditions (Wierenga et al., 1993). Titanium was chosen because it is highly resistant to dissolution and has excellent 7wetting properties. Once the porous Ti plate is water-saturated, water but not air is allowed to flow-through the 0.2 μm pores, as long as the applied pressure differential does not exceed the air entry relief pressure, referred to as the bubble pressure, of the Ti plate. If the pressure differential is exceeded, air will escape through the plate and compromise the ability to maintain unsaturated flow conditions in the column. The PUF test computer control system runs LabVIEW™ (National Instruments Corporation) software for logging test data from several thermocouples, pressure sensors, inline sensors that measure effluent pH and conductivity, and from an electronic strain gauge that measures column weight to accurately track water mass

balance and saturation level. The column also includes a PUF port, which is an electronically actuated valve that periodically vents the column gases. The purpose of column venting is to prevent reduction in the partial pressure of important gases, especially O_2 and CO_2, which may be consumed in a variety of chemical reactions.

The PUF column for the waste form-waste form interaction experiment was packed first with approximately one-half the total required SRL-202 glass (12.87 g), then with the LaBS glass (8.64 g), and finally with the remaining SRL-202 glass (13.65 g) (Fig. 2). This resulted in a packed PUF column that contained approximately 80% SRL-202 glass and 20% LaBS glass. The mass difference between the full and empty column was used to calculate the initial porosity of approximately 0.44 ± 0.03 (unitless). Mass change and bed volume were also tracked while packing each layer to compute the porosity of each layer. Individual bed porosity was within the experimental uncertainty of the measurement reported above. After packing, the column was vacuum saturated with 18 MΩ DIW at ambient temperature. A temperature controller was then programmed to heat the column to 90 °C(±2 °C) in approximately 1 h (1 °C/min). The column initially was allowed to desaturate by gravity drainage during heating and was also vented periodically to maintain an internal pressure less than the bubble pressure of the porous plate. After reaching 90 °C(±2 °C), the DIW influent valve was opened and influent was set to a flow rate of 1 mL/day. The influent solution, 18 MΩ DIW, was stored in a sealed 50 mL influent reservoir which was periodically refilled during the experiment. Column venting was set to occur once per hour, so that the partial pressure of O_2 and CO_2 could remain relatively constant.

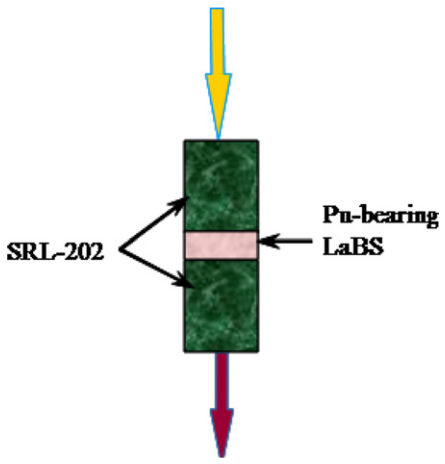

Fig. 2. Schematic of the column setup for PUF waste form/waste form interaction experiment.

3.1. Effluent solution analyses

All effluent solutions were monitored for pH and electrical conductivity with in-line sensors. Prior to starting the experiments, the in-line pH probe was calibrated with NBS buffers (pH 7.00, 10.00, or 12.00 at 25 °C). Precision of pH measurement was ±0.02 pH units. The in-line Pharmacia Biotech electrical conductivity sensor was calibrated with a freshly made solution of 1.0 M NaCl. The 1.0 M NaCl solution was prepared by adding 11.67 g of analytical grade NaCl powder to 200 mL of 18 MΩ DIW. Concentrations of Gd, La, Nd and Pu in effluent solution samples were determined with ICP-MS methods; whereas concentrations of Al, B, Cr, Fe, K, Li, Na, Si, Ti and Zr were determined with ICP-OES methods. After passing through the 0.2 μm Ti porous plate and the inline sensors, aliquots of the effluent solutions were acidified with ultra high-purity concentrated HNO_3 and analyzed by ICP-MS and ICP-OES methods.

3.2. Post-test solid phase analyses

After 2158 days (approximately 6-a), the PUF experiment was terminated. Upon termination, the column was vertically split into two halves, and the reacted solids were sub-sampled as found (loose and moist particles) as a function of depth (2–3 mm intervals). The sub-samples were placed in glass vials, dried at room temperature in a sealed container with $CaSO_4$ desiccant, and analyzed for secondary reaction products with X-ray diffraction (XRD), scanning electron microscope (SEM), and alpha energy analysis (AEA).

Powder XRD patterns were recorded in a Scintag® automated powder diffractometer (Model 3520) with Cu K_α radiation X-ray tube ($\lambda = 1.54$ Å). Data were collected in the 2θ range: 2–65°, with a scanning step size of 0.02° 2θ and a dwell time of 2 s. Before mounting, a representative sample of the bulk material was ground with an agate mortar and pestle and sealed in a specialized XRD holder (Strachan et al., 2003). The data were analyzed with the computer program JADE

(MDI, Livermore, California) combined with the Joint Committee on Powder Diffraction Standards (JCPDS) International Center for Diffraction Data (ICDD) (Newtown Square, Pennsylvania) database.

A JEOL JSM-840 SEM was used to determine particle morphology and size. The system is equipped with an Oxford Links ISIS 300 energy dispersive X-ray analysis spectroscopy (EDS) that was used for qualitative elemental analysis. Operating conditions were 20 keV for SEM imaging, and 100 live seconds with 20–30% dead time for the EDS analyses. The EDS analyses of particles are limited to elements with atomic weights heavier than B. Photomicrographs of high-resolution secondary electron images were obtained as digital images and stored in electronic format. The SEM-EDS mounts consisted of double-sided C tape attached to a standard Al planchet. The sample mounts were then coated via vacuum sputtering to improve the conductivity of the samples, and thus, the quality of the SEM images and EDS signals.

The distribution of ^{239}Pu and ^{241}Am as a function of column depth was determined by analyzing samples of reacted particles with an Oxford Oasis^{TM} Alfa Energy Analysis (AEA) system that contains eight individual alpha detectors. This distribution was used to evaluate how far, if at all, Pu has migrated into the bottom half of the SRL-202 glass bed. All detectors were energy and efficiency calibrated for a distinct geometry using standards with known activities of analyzed isotopes. Identification of ^{239}Pu and ^{241}Am spectra was performed with the 5.156 MeV peak and 5.486 MeV peak, respectively.

4. Quantification of the elemental release rates and glass dissolution rates

The elemental release rates from the PUF column, based on the concentration of elements measured in the effluent solution samples, were determined by the following formula:

$$E_{r_{i,j}} = \frac{4\varepsilon q(c_{i,j,L} - c_{i,j,b})}{\theta S_{\mathrm{geo},j}(1-\varepsilon)\rho\pi d^2 L} \quad (2)$$

where r_i is the elemental release rate of the ith element [mol/(m^2 s)], $c_{i,jL}$ is the effluent concentration of the ith element released from the jth glass (mol/L), c_{ijb} is the background concentration of the ith element released from the jth glass (mol/L), d is the column diameter (m), L is the column length (m), q is the volumetric flow rate (L/s), $S_{\mathrm{geo},j}$ is the specific surface area for the jth glass, ε is the porosity (unitless), ρ is the glass density (kg/m^3), and θ is the volumetric water content (unitless). Although the majority of the elements exiting the PUF column are present in only one glass, five elements (Al, B, Nd, Si and Zr) are contained in both glasses. For these five elements, an average particle density ($\rho = 3.13 \times 10^3$ kg/m^3) and geometric surface area ($\overline{S}_{\mathrm{geo}} = 3.7$ m^2/kg) was used to compute the elemental release rates. The volumetric water content is calculated based on the mass of a volume of water in a fixed column volume, accounting for changes in the solution density resulting from temperature changes. The background concentration for most elements is typically below the estimated quantification limit (EQL) for the respective analysis. The EQL is defined as the lowest calibration standard that can be determined reproducibly during an analytical run within 10% of the certified value multiplied by the sample dilution factor. The lowest EQLs were for La (from 0.2 to 1 μg/L), Gd (from 0.2 to 1 μg/L), Nd (5 μg/L) and Pu (from 0.002 to 0.2 μg/L). Higher EQLs were found for Cr (62.5 μg/L) and Ti (50 μg/L), with the EQLs being the highest for K (1000 μg/L), Na (1000 μg/L), Li (10,000 μg/L) and Si (10,000 μg/L). In cases where the analyte is below the EQL, the background concentration of the element is set at the value of the EQL. The elemental release rate allows for a comparison of the release behavior of each element exiting the PUF column, without normalizing the elements based on the composition of the glass.

Unlike the elemental release rate, glass dissolution rates, based on the concentration of elements in the effluent, were normalized to the amount of the element present in the glass specimens and determined by

$$r_{i,j} = \frac{E_{r_{i,j}} M_i 86400}{f_{i,j}} \quad (3)$$

where r_i is the glass dissolution rate based on the ith element released from the jth glass [g/(m^2 d)], $E_{r_{i,j}}$ is the elemental release rate [mol/(m^2 s)], f_i is the mass fraction of the ith element released from the jth glass (unitless), and M_i is the molecular weight of the ith element (g/mol).

An estimate of the 2σ experimental uncertainty for the elemental release and glass dissolution rates were determined with error propagation. For additional details on the error propagation equation for PUF experiments see Pierce et al. (2006).

5. Results and discussion

5.1. Computer-monitored test metrics

Results from the computer-monitored test metrics, volumetric water content (θ), pH, and electrical conductivity (Ω), are shown in Fig. 3. The sensor data were smoothed using a bi-square weighting method where the smoothed data point, y_s, is given by $y_s = (1 - \omega^2)^2$. The parameter ω is a weighting coefficient calculated from a window surrounding the smoothing location in the set of the independent variables. A low-order polynomial regression (order 2 in this case) is used to compute ω for each smoothed value. The smoothed data are provided as lines and were used to make qualitative assessments of the results Fig. 3.

The volumetric water content (θ) results illustrate that, although there were minor excursions during this experiment, the volumetric water content (θ) was relatively steady until day 1500. From day 1500 until the test was terminated, the volumetric water content increased steadily, going from an average of 0.26 ± 0.02 to 0.34 ± 0.01. This is due to changes in the columns hydraulic properties caused by an increase in secondary reaction products, as well as an increase in the waters of hydration associated with these phases. The formation of fine-grained phases causes the water-retention to increase as well as the hydraulic conductivity and rate of water flow through the column to decrease, thereby causing the water content to increase as seen in Fig. 3a. This trend has also been observed in the early stages of a PUF test with a less-durable glass formulation, LD6-5412, (McGrail et al., 1999). McGrail et al. (1999) measured the hydraulic conductivity as a function of PUF test duration with the unsaturated flow apparatus

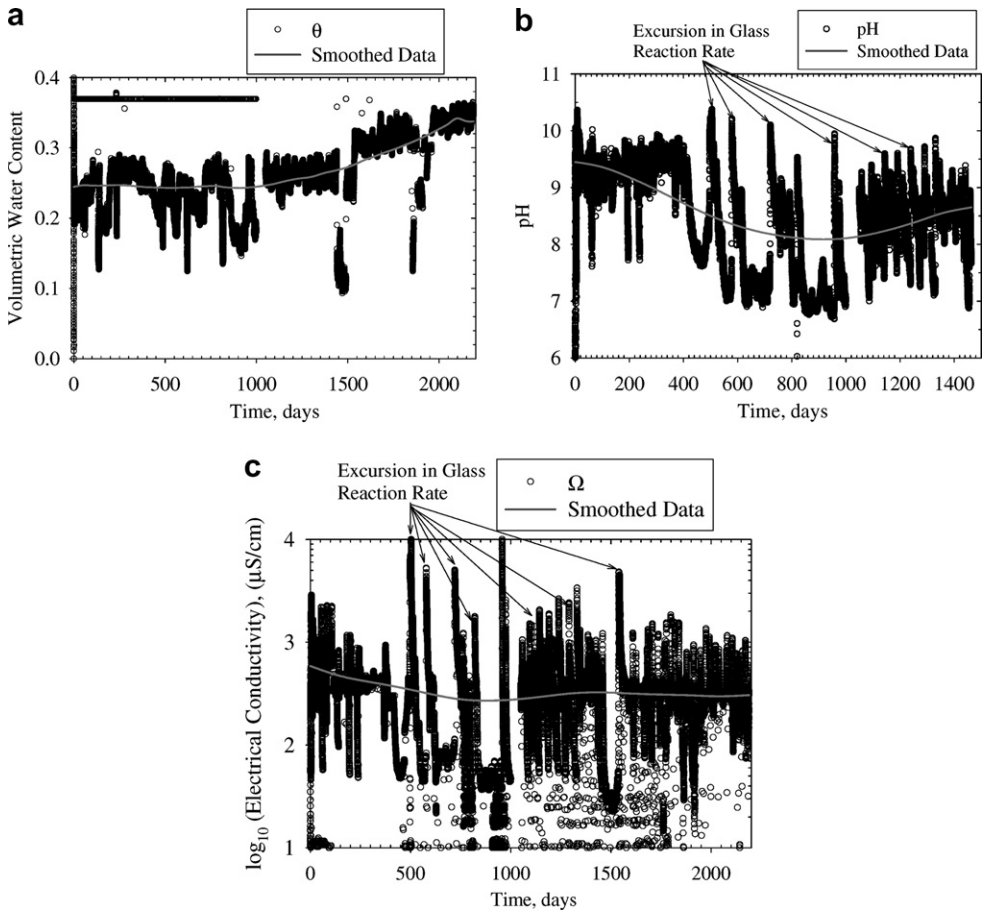

Fig. 3. Computer-monitored test metrics for the volumetric water content (a), pH (b) and electrical conductivity (c). The grey lines are the bi-squared smoothed fit of the raw data and are provided as a guide to the eye.

(UFA) (Conca and Wright, 1992; Gamerdinger and Kaplan, 2000). The results from McGrail et al. (1999) illustrated that changes in the water-retention characteristics of the hydrated glass are manifested as an increase in the volumetric water content during a PUF test and this increase is related to the initial precipitation of the zeolitic alteration phases, phillipsite ($KCaAl_3Si_5O_{16}$) and gobbinisite ($Na_4CaAl_6Si_{10}O_{32} \cdot 12H_2O$).

Unlike the volumetric water content, pH and electrical conductivity (Ω) excursions occur much more frequently (Fig. 3b and c). Note the pH probe was lost after day 1400; consequently, data beyond this point are not available. A direct comparison of available pH, electrical conductivity, and solution chemistry data suggest that these data excursions are correlated to chemical changes occurring at the glass-water interface. These changes can cause the glass reaction rate to increase by orders of magnitude. For example, it has been shown in flow-through experiments that an increase in pH, from 9 to 10, causes an order of magnitude increase in the reaction rate of aluminoborosilicate glasses (McGrail et al., 1997b; Pierce et al., 2004).

5.2. Effluent solution chemistry

Results from the analyses of effluent samples are provided in Fig. 4 and represent the release of elements from the PUF column as a whole and not from an individual glass specimen. Release of elements from the column illustrates a general trend of decreasing concentration with increasing reaction time during the early stages of the test (first 200 days). The concentrations of B, K, Li, Na and Si are as much as 1×10^5 times greater than Al, Cr, Fe, Nd, Ti and Zr (Fig. 4a, b and c). Fig. 4c also illustrates that release of Gd, La and Pu from the LaBS glass ranged from as little as 1×10^3 to as much as 1×10^8 times lower than the other elements. Under these conditions, B, K, Li and Na are more soluble than Al, Cr, Fe, Nd, Ti and Zr and much more soluble than Gd, La, and Pu. The high concentration of Pu observed in these effluent samples is the result of colloidal particles exiting the column. Results from alpha energy analysis (AEA) of aliquots of select effluent samples that were filtered through a 1.8 nm filter suggest that approximately 80% of the total measurable Pu was in the form of

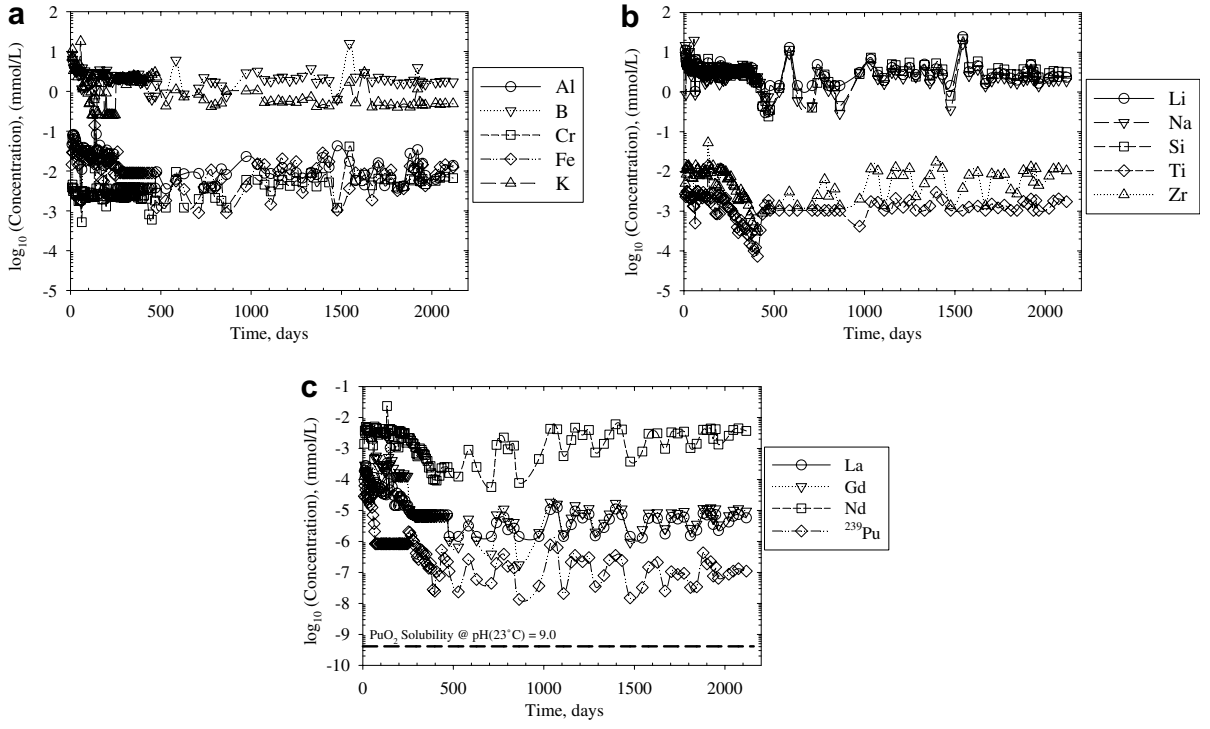

Fig. 4. Log_{10} concentration of elements, in mmol/L, released from the PUF column measured in effluent solutions as a function of time, in days. The Pu concentration in equilibrium with PuO_2 at pH (23 °C) = 9.0 is shown as a dashed horizontal line in (c). Five of the elements; Al, B, Nd, Si and Zr, shown in the above plots are being released from both glasses.

a filterable particulate, in comparison to unfiltered aliquots of the same sample. These results suggest the filterable particles are >1.8 nm but smaller than the 0.2 μm average diameter openings of the Ti porous plate situated at the base of the column. This is consistent with PUF (McGrail et al., 2000a) and PCT (Ebert and Bates, 1993) tests conducted on Pu-bearing ceramic and glass, respectively. Ebert and Bates (1993) observed Pu-bearing colloidal particles that were approximately 1.8 nm in size. Transport of colloids in a PUF test is to be expected, because the system is advection dominated. This can be demonstrated by calculating a Peclet (P_e) number for this experiment with Eq. (4);

$$P_e = \frac{\left(\frac{q}{\theta A}\right)x}{D}, \quad P_e > 4 \text{ (advection-dominated system)} \tag{4}$$

where q is the flow rate (1.2×10^{-11} m/s), θ is the average volumetric water content, which changed from 0.26 ± 0.02 to 0.34 ± 0.01, A is the column area (2.85×10^{-4} m^2), x is the column distance (0.0762 m), and D is the molecular diffusion coefficient for water (assumed to be 1.0×10^{-9} m^2/s). This calculation resulted in an average P_e number of 10.5 ± 2. This value clearly shows that this PUF test is advection-dominated.

Despite the highly advection-dominant system, the steep ^{239}Pu and ^{241}Am concentration gradient downstream from the LaBS glass indicates a strong attenuation of Pu at the lower LaBS/SRL-202 glass interface, evident by the 5-order-of-magnitude drop in the measured activity over a distance of 10 mm (Fig. 5). Retention of Pu may be occurring by any number of or a combination of factors such as: (1) adsorption from solution onto colloidal particles, (2) colloid filtration (e.g., entrapment of Pu-bearing colloids in the lower SRL-202 glass beads), and/or (3) formation of Pu-bearing secondary phases. Although it is impossible to distinguish these mechanisms from the AEA data alone, most of the Pu exiting the column was colloidal and suggests colloid filtration may be the retention mechanism causing the dramatic drop in ^{239}Pu activity.

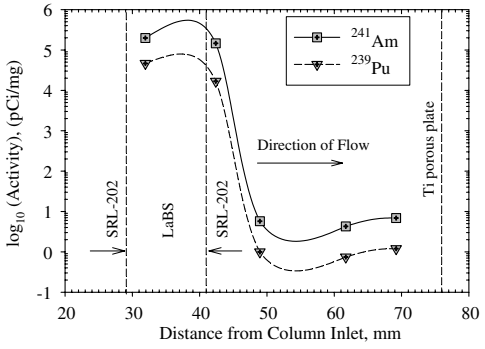

Fig. 5. Alpha energy analysis (AEA) of glass particles removed from PUF column after 6-a of reaction.

A comparison of Figs. 3 and 4 illustrates good correlation between the observed excursions in effluent pH and electrical conductivity with peak concentrations of constituents released from the PUF test. These results suggest the SRL-202 glass, and perhaps the LaBS glass, have undergone periodic excursions in reaction rates. However, a majority of the elements contained in the LaBS glass are sparingly soluble under these test conditions, so it is highly unlikely that a dissolution rate acceleration of the LaBS glass could cause the transients in pH and electrical conductivity. Periodic excursions in the effluent pH and electrical conductivity have been observed in previous PUF tests with the SRL-202 glass, as well as with other glass formulations, and have been correlated with the formation of secondary phases, especially Na–Ca aluminosilicate zeolites (McGrail et al., 1999, 2000a; Pierce et al., 2006).

5.3. SRL-202 and LaBS glass elemental release rate

A comparison of the elemental release rates, Eq. (2), for the major and a few minor components in SRL-202 and LaBS glasses is shown in Fig. 6. Similar to the concentration data, the rate of element release from the column decreases as the reaction time increases, especially during the early stages of testing (Fig. 6). The most significant decrease is observed during the first year of testing, followed by periodic increases in the elemental release rate. The decrease in the rate of element release suggests the value of the ion activity product is approaching equilibrium with respect to a rate-limiting secondary phase. Over the 6-a testing period, the overall release of elements from the PUF column has decreased and reached an average steady-state release rate, based on B release, of $(2.87 \pm 0.27) \times 10^{-10}$ mol/(m^2 s), excluding the periodic excursions in reaction rate. The results in Fig. 6 were also used to determine the average rate of SRL-202 glass dissolution, based on Li release, with Eq. (3). The calculated rate for the SRL-202 glass was estimated to be $(1.22 \pm 0.18) \times 10^{-2}$ g/(m^2 d) (Fig. 7). This rate is 8.3 times greater than a rate previously reported by

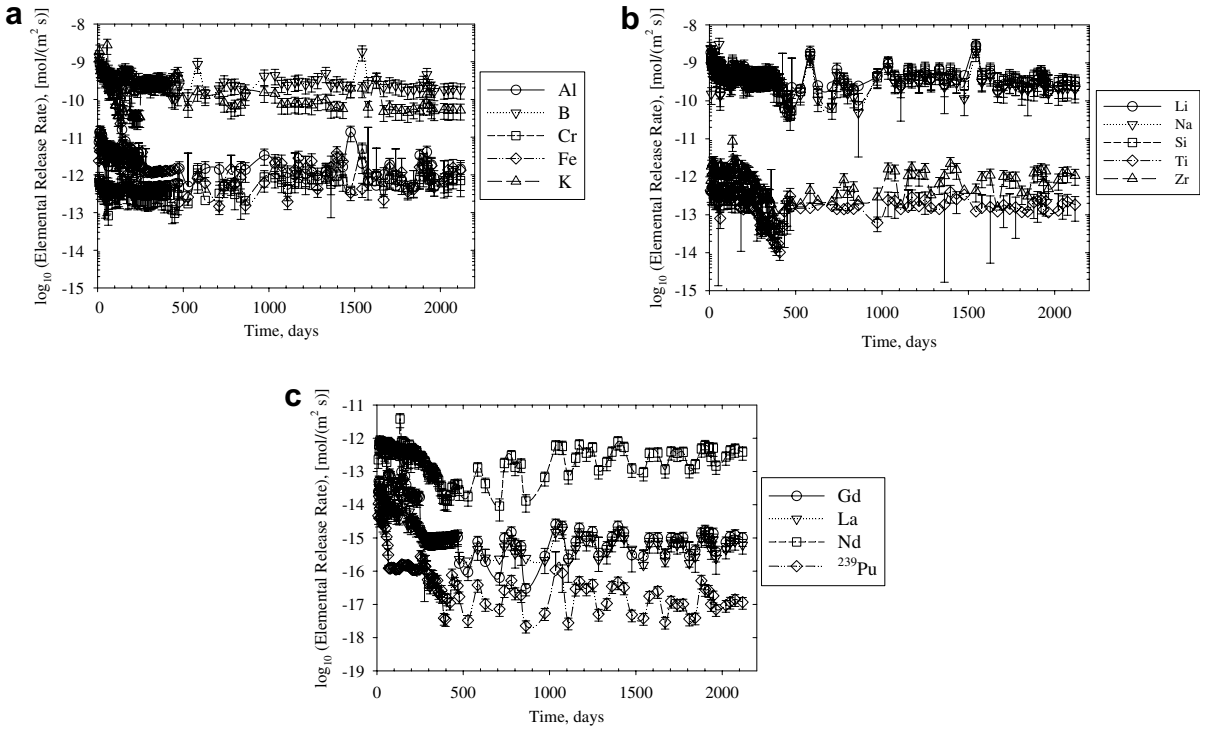

Fig. 6. Element release rates, in mol/(m^2 s), from both SRL-202 and LaBS glasses as a function of time is shown in (a–c). Five of the elements; Al, B, Nd, Si and Zr, shown in the above plots are being released from both glasses.

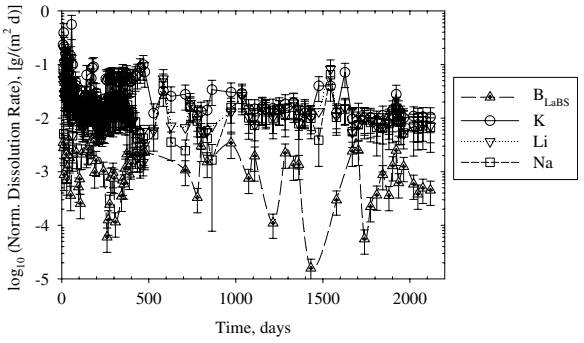

Fig. 7. Glass dissolution rate, in g/(m^2 d), as a function of time is shown for B_{LaBS}, Li, K and Na. The dissolution of SRL-202 glass is represented by the normalized release of the alkali elements (K, Li and Na) whereas, LaBS glass dissolution was estimated by difference and is represented by B_{LaBS}.

McGrail et al. (1997a) after a 70-day PUF test with SRL-202 glass, $(1.47 \pm 0.13) \times 10^{-3}$ g/(m^2 d). The present results suggest that the presence of LaBS glass may be causing the SRL-202 glass to dissolve faster than previously observed and may be the result of changes in the solution chemistry that occur as the water migrates first through SRL-202 glass bed, to the LaBS glass bed, and finally through another SRL-202 glass bed during this waste form-waste form interaction PUF column.

Although the release of alkali elements (i.e., K, Li, and Na) from glass can occur via two mechanisms, matrix dissolution and alkali-H^+ ion exchange (Bates et al., 1994a,b). It has been illustrated in single-pass flow-through test (SPFT) and PUF test with LAW glass, (conducted at 90 °C and a pH (23 °C) > 9.0) that matrix dissolution is the dominant reaction mechanism, and the process of alkali-H^+ ion exchange is negligible (McGrail et al., 2001; Pierce et al., 2004, 2006).

5.4. LaBS glass dissolution rate

An estimate of the LaBS glass dissolution rate in this waste form-waste form interaction PUF test was determined by subtracting the SRL-202 glass average normalized Li release rate ($r_{Li,SRL\text{-}202}$) from the average normalized B release rate [measured by total B release, $(1.24 \pm 0.05) \times 10^{-2}$ g/(m^2 d)] and multiplying by the ratio of LaBS to SRL-202 mass fractions for B [Eq.].

$$r_{B,\mathrm{LaBS}} = \left(\frac{E_{r_{B,\mathrm{Total}}} M_B 86400}{f_{B,\mathrm{SRL\text{-}202}}} - r_{\mathrm{Li,SRL\text{-}202}}\right)\left(\frac{f_{B,\mathrm{SRL\text{-}202}}}{f_{B,\mathrm{LaBS}}}\right) \quad (5)$$

With this approach, the average normalized B release rate for the LaBS glass (B_{LaBS}) was estimated to be $(1.22 \pm 0.14) \times 10^{-3}$ g/(m^2 d). The measured rate for LaBS glass is 10 times lower than for SRL-202 glass; similar results have been observed when comparing rates from static tests (Fortner et al., 2000; Mertz et al., 1998). A comparison of the rates as a function of time for SRL-202 glass; indicated by the release of K [$(2.37 \pm 0.18) \times 10^{-2}$ g/(m^2 d)], Li [$(1.22 \pm 0.18) \times 10^{-2}$ g/(m^2 d)], and Na [$(1.08 \pm 0.11) \times 10^{-2}$ g/(m^2 d)], and LaBS glass, indicated by B_{LaBS} release, is shown in Fig. 7. A comparison of the average LaBS glass dissolution rate based on B_{LaBS}, suggests that Gd [$(1.87 \pm 0.17) \times 10^{-7}$ g/(m^2 d)], La [$(8.27 \pm 0.95) \times 10^{-8}$ g/(m^2 d)], and Pu [$(5.03 \pm 1.39) \times 10^{-9}$ g/(m^2 d)] are being retained in the column, either as a discrete secondary phase(s) or via adsorption and/or absorption with secondary phases formed as a result of the glass-water reaction. Since Gd, La and Pu are sparingly soluble the reported dissolution rates based on these elements, are used to compare the relative magnitude of release from the PUF column in comparison to B_{LaBS} and is not indicative of the dissolution rate for LaBS glass.

5.5. Analysis of reacted SRL-202 glass particles and geochemical modeling

The moisture associated with reacted glass particles removed from the PUF column is shown in Fig. 8 as a function of depth. Results suggest the volumetric water content for each column section decreases with depth away from the column inlet and the most extensive secondary phase formation (and consequent glass degradation) occurred near the column inlet, evident by the peak in water content for these particles. Analysis of the reacted grains at various depths with SEM confirmed that samples removed from the top of the column had the most extensive alteration. Figs. 9 and 10 illustrate the presence of a gel layer and numerous particles with a spherical morphology. Here the term gel layer refers to a hydrolyzed layer on the glass surface that forms as a result of condensation reactions that occur at the glass-water interface. The EDS analyses of the spherical particles indicate the presence of Al, K, Ca, Fe, Mg, Mn, Ni and Zr; but in comparison to the pristine glass, these spherical particles are enriched in Al, Fe, and Si, with a small amount of Na. The presence of these spherical particles is not surprising and has been observed in previous PUF tests with the SRL-202 glass conducted for shorter durations (McGrail et al., 1997a). Further examination of these images suggests that some of these particles are embedded and probably growing out of a gel layer (Fig. 10).

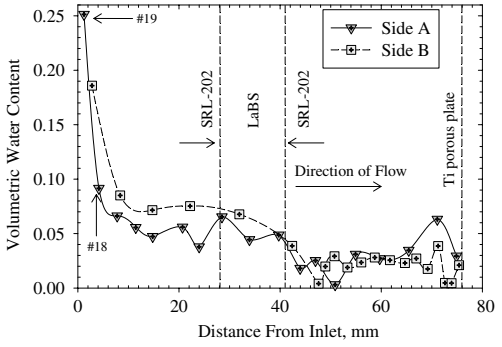

Fig. 8. Moisture fraction as a function of distance from the PUF column inlet.

In addition to SEM-EDS analyses, powder XRD and geochemical modeling was used in an attempt to characterize the secondary phase(s) that precipitated in the PUF column. The bulk powder XRD results shown in Fig. 11 suggest the secondary phase present in the SEM images may be the smectite di-octahedral clay mineral nontronite [$Na_{0.33}Fe_2(AlSi)_4O_{10}(OH)_2 \cdot n(H_2O)$], although the 100% reflection (e.g., 9.2 2θ) for nontronite was not observed. Typically, XRD requires the presence of 5 wt% or more for detection. To provide additional support for the presence of nontronite, the saturation state of the effluent solutions with respect nontronite was evaluated with geochemical modeling. Applying geochemical modeling, with the thermodynamic database and reaction code EQ3NR [version 8.0 (Wolery, 1992)], to the measure concentration of elements in select effluent samples and allowing the hypothetical solid solutions to precipitate, suggests these samples are super-saturated with respect to two smectite di-octahedral clays, nontronite and beidellite [$Na_{0.33}Al_{2.33}Si_{3.67}O_{10}(OH)_2$].

5.6. Analysis of reacted LaBS glass particles

SEM images (Fig. 12) and X-ray EDS analyses of reacted LaBS glass confirmed the presence of a discrete Pu-bearing secondary phase, probably PuO_2,

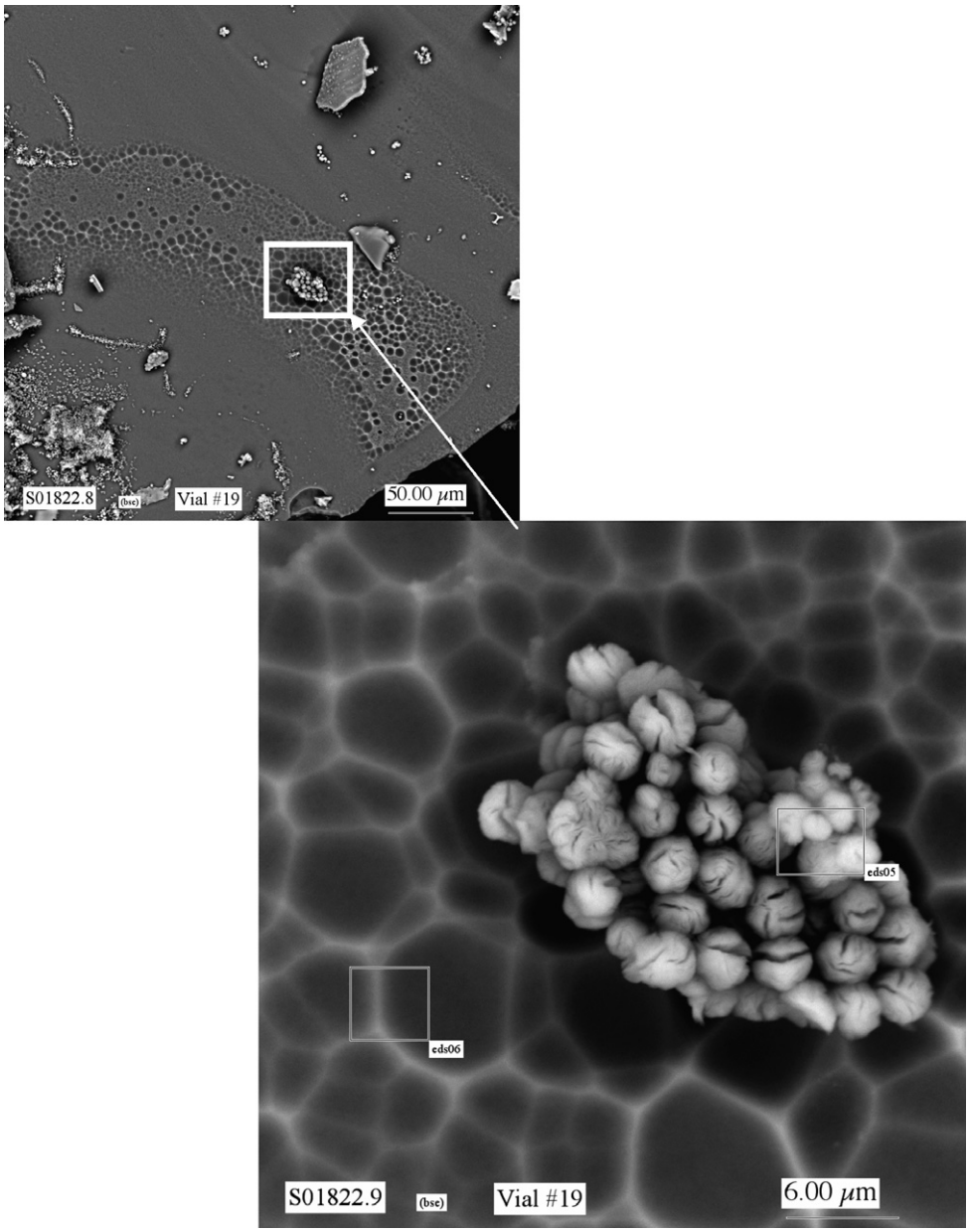

Fig. 9. SEM photographs of reacted SRL-202 glass particles removed from the top of the PUF column (between 4 and 8 mm from the top). A smectite-di-octahedral clay phase is shown as spherical particles growing out of a hydrated gel layer on the SRL-202 glass grains. X-ray EDS analyses (eds05) suggest these particles are enriched in Al, Fe and Si, with a small amount of Na; in comparison to the pristine glass; where as the hydrated gel layer (eds06) contains majority of the SRL-202 glass components.

which was the predicted secondary phase that formed when modeling the effluent solution chemistry with the EQ3NR code (Wolery, 1992). Numerous deposits with a plate-like morphology were found on glass particles removed from a column depth between 32 and 34 mm. These particles have a high Pu content, do not contain any of the other major LaBS glass components (i.e., Al, Gd, La, Nd and Si), and appear to have precipitated on the surface of the LaBS glass. Alteration products that contain the neutron absorber, Gd, have not been positively identified. Gadolinium is expected to form insoluble secondary phases after being released from the glass. Therefore, the separation

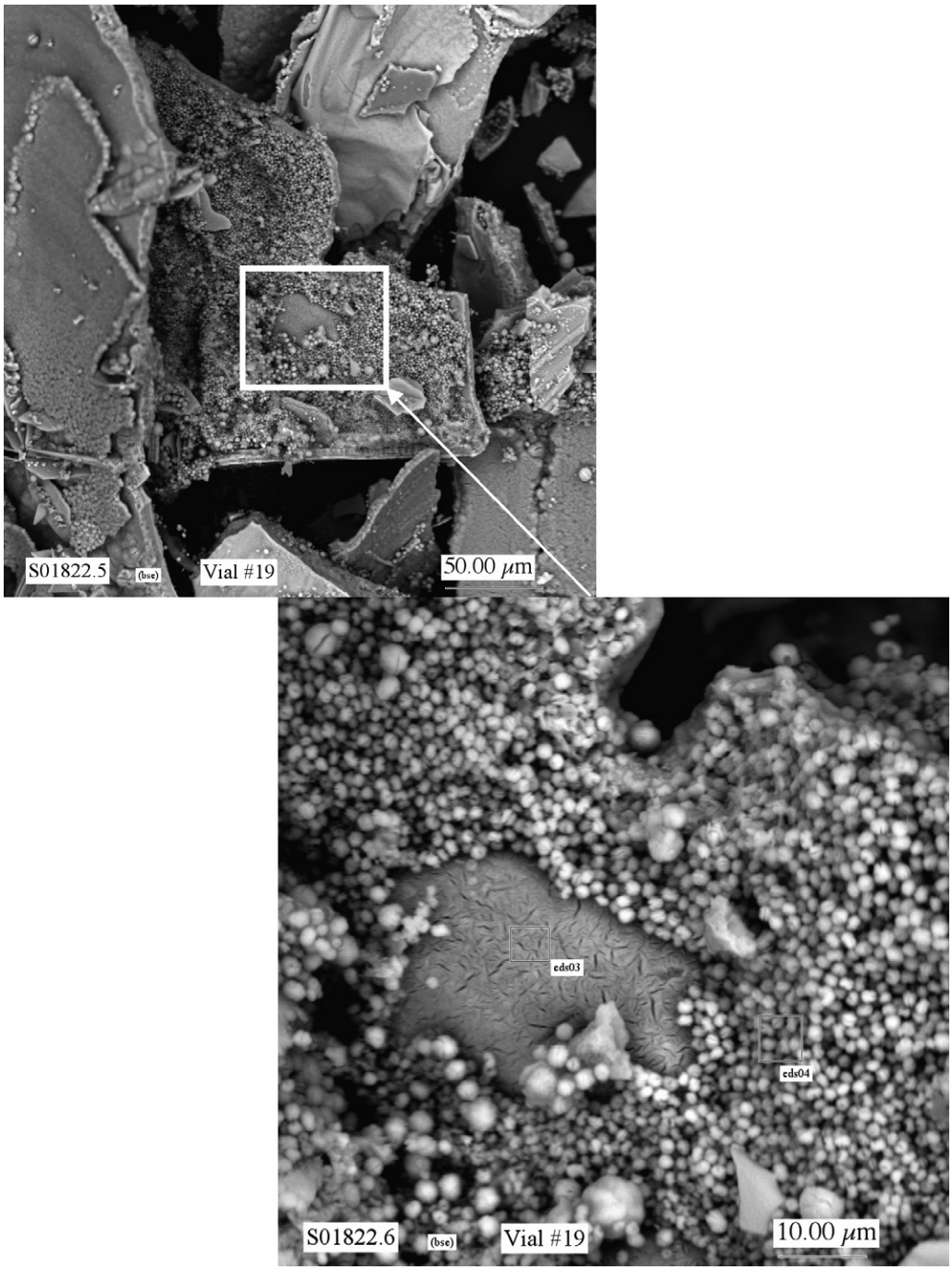

Fig. 10. SEM photographs of reacted SRL-202 glass particles removed from the top of the PUF column (between 4 and 8 mm from the top). A large number of particles with a spherical morphology have accumulated on the surface of the glass particles. The EDS analyses (eds04) suggest these particles mainly contain Al, Fe, K and Si, with trace amounts of Ca, Mn, Mg, Ni, Ti and Zr. The hydrated gel layer in the center (eds03) is enriched in Al, Fe, K and Si in comparison to the spherical particles.

of this neutron absorber from Pu during LaBS glass dissolution and transport could be a criticality issue for the proposed repository. Previous studies (Bates et al., 1995; Fortner et al., 2000; Mertz et al., 1998) have shown the formation of individual and adhered Pu-bearing colloids, but none have shown

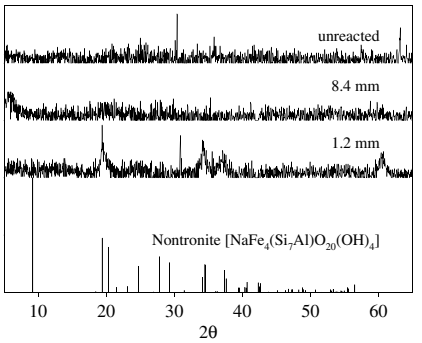

Fig. 11. Background-corrected XRD pattern of reacted SRL-202 glass particles taken between 0 and 9 mm from the top of the PUF column, unreacted glass, and the nontronite PDF pattern for comparison.

the segregation of Pu from the neutron absorbers. For example, a 98-day PCT-B test conducted by Fortner et al. (2000) revealed that Pu was associated with secondary phases of oxides, oxyhydroxides and silicates of Gd, La and Nd. It is very difficult to compare the present results to results obtained in other studies because of differences in the test designs and methods used. Currently, it is not clear why Pu appears to have segregated from the neutron absorber, and additional analysis is required to translate these results to actual disposed waste packages.

Recent unpublished results from a fabrication conducted with a new LaBS glass formulation that contains both Gd and Hf at Savannah River National Laboratory (SRNL) suggest the LaBS glass used in the present study may have contained an insoluble Pu phase that was not dissolved during the glass fabrication process (James Marra, pers. comm.). Vienna et al. (1996) observed undissolved Pu when the sample was not stirred during the melting process. The stirring technique was used during fabrication of the LaBS glass in the present study, but similar techniques were not used at SRNL. Based on the unpublished results from SRNL, it is possible that the disk-like Pu-bearing phase(s) observed in the reacted glass may have been present in the unreacted glass prior to being used in the PUF test, although the Pu phase was not observed in SEM images of the unreacted LaBS glass.

5.7. Analysis of Pu release from LaBS glass

A one-dimensional (1-D) steady-state mass balance equation, Eq. (6), was used to predict the depth at which the Pu concentration approaches saturation with respect to PuO_2. The governing equation for describing 1-D chemical transport assuming a constant volumetric water content and flow-rate at steady-state is given by:

$$D\frac{\partial^2 c_i}{\partial x^2} - v\frac{\partial c_i}{\partial x} + \gamma = 0 \tag{6}$$

where D is the dispersion coefficient in $\mathrm{m\,s^{-1}}$ (1.16×10^{-14} m/s), c_i is the concentration of element i in $\mathrm{g/m^3}$, v is the interstitial or pore-water velocity ($1.35\times10^{-7}\ \mathrm{m^3/s}$), and γ is the source release term in $\mathrm{g/(m^3\,s)}$. The pore-water velocity is equal to the flow rate ($q = 1.16\times10^{-11}\ \mathrm{m^3/s}$) divided by the average volumetric water content for the entire experiment ($\theta = 0.30 \pm 0.01$), which was computed by averaging the observed volumetric water content from day 1 to day 1500 and from day 1500 until test termination, 0.26 ± 0.02 and 0.34 ± 0.01, respectively. The source release term, γ, $1.66\times10^{-4}\ \mathrm{g/(m^3\,s)}$ was calculated for the LaBS glass by multiplying the average steady-state dissolution rate, based on B release, [$r_{\mathrm{LaBS}} = (1.22 \pm 0.14)\times10^{-3}\ \mathrm{g/(m^2\,d)}$] times the surface area ($S_{\mathrm{LaBS}} = 2.77\times10^{-2}\ \mathrm{m^2}$) to bed volume ($V_{\mathrm{LaBS}} = 4.34\times10^{-6}\ \mathrm{m^3}$). Applying a boundary condition of $c(0) = c_{i,o}$ and $\frac{\partial c}{\partial x}(L) = 0$, the resulting analytical solution for Eq. (6) from van Genuchten and Alves (1982) is:

$$c_i(x) = c_{i,o} + \frac{\gamma x}{v} + \frac{\gamma D}{v^2}\left\{\exp\left(-\frac{vL}{D}\right) - \exp\left[\frac{(x-L)v}{D}\right]\right\} \tag{7}$$

where $c_i(x)$ is the concentration of element i at a set column depth in $\mathrm{g\,m^{-3}}$, $c_{i,o}$ is the initial concentration of element i in $\mathrm{g\,m^{-3}}$, and L is the total column length extending from the column top through the LaBS glass bed, approximately 15 mm. Using Eq. (7), the predicted Pu concentration was calculated in 0.04 mm intervals. Because of the observed pH fluctuations (see Fig. 3b) and the fact that PuO_2 solubility decreases with increasing pH (Allard and Rydberg, 1983; Rai et al., 1999, 2001), a conservative experimental pH value of 9.0 was used to predict the boundary condition for the solubility of PuO_2 using the EQ3NR code (Wolery, 1992). Numerically solving Eq. (7) for x using the pH (23 °C) = 9.0 restriction, the concentration of Pu is predicted to exceed the PuO_2 solubility at approximately 29.0 mm. Although these results suggest the solubility of PuO_2 is exceeded soon after the LaBS glass begins to corrode, in dynamic experiments such

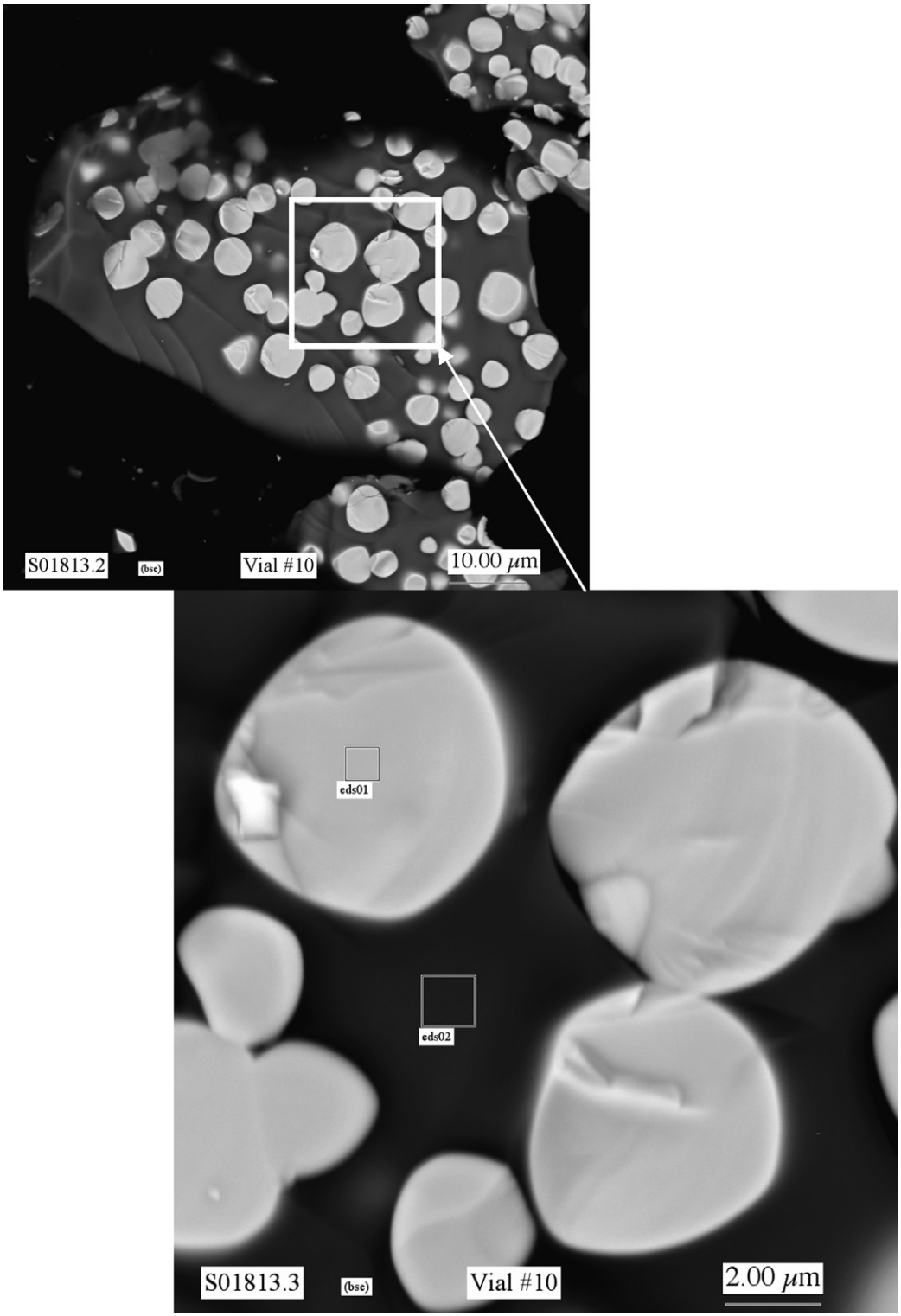

Fig. 12. SEM photograph of reacted LaBS glass particles removed from the center of the PUF column (between 32 and 34 mm from the top). X-ray EDS analyses suggest that the disk-like phase is enriched in Pu (possible PuO_2) and devoid of the other LaBS glass components (Al, Gd, La, Nd and Si).

as these, the amorphous analog usually forms earlier than the crystalline phase. These thermodynamic calculations are based on the solubility product (K_{sp}) for the crystalline parent, which is always lower than that of the amorphous analog. This predicted depth is within 3 mm of the insoluble Pu-bearing phase(s) present on the LaBS glass reaction products removed from a column depth between 32 and 34 mm (see Fig. 12). These calculated results provide additional confirmation that the majority of the Pu released from the corroding glass was retained in the region of the LaBS glass bed.

6. Conclusions

In a 6-a long PUF experiment, a simulated HLW glass, SRL-202, and LaBS glass for Pu immobilization have been allowed to react in a manner similar to the way they might react in a repository. The results from this experiment have provided several important insights into the long-term release behavior of Pu and neutron absorbers from the LaBS glass. The results show a strong coupling between the chemistry of the water percolating through a porous media of the test materials and the corrosion rate of the LaBS glass. Consequently, should the HLW glass undergo sustained acceleration in its corrosion rate due to secondary phase formation, the resulting excursion in pH could significantly impact the corrosion rate of the LaBS glass. The 2–3 pH unit transient excursions observed in the solution pH exhibited over the entire course of this PUF experiment are probably caused by the transient acceleration in the glass corrosion rate from the formation of alteration phases. These excursions cause as much as a two order-of-magnitude increase in the B release rate from the PUF column. Comparison of the corrosion rate after 70 days of testing, suggests the SRL-202 glass is experiencing reaction rate acceleration in this waste form-waste form interaction PUF test, which is evident by the one to two orders-of-magnitude increase in the dissolution rate. This reaction rate acceleration is almost certainly due to the formation of a smectite di-octahedral clay, probably nontronite $[Na_{0.33}Fe_2(AlSi)_4O_{10}(OH)_2 \cdot (H_2O)]$ or beidellite $[Na_{0.33}Al_{2.33}Si_{3.67}O_{10}(OH)_2]$, as well as changes to the solution chemistry at the SRL-202-LaBS glass interface. As water interacts with the top layer of SRL-202 glass, it becomes saturated with respect to the SRL-202 glass components and reaches a steady-state pH. In this representative can-in-canister (i.e., sandwich) column configuration, this same volume of water is undersaturated with respect to several major components contained in the LaBS glass, such as Gd, La, Nd and Pu. As these components are dissolved, the solution chemistry changes and reaches a new steady-state pH. Finally, the solution interacts with the bottom layer of SRL-202 glass, causing an additional change in the solution chemistry. This final shift in the solution chemistry is expected to be less dramatic than the changes that occurred in the upper layer of SRL-202 glass. These shifts in the solution chemistry have a profound effect on the dissolution of the SRL-202 and LaBS glasses.

Alpha energy analysis (AEA) of aliquots of select effluent samples that were filtered through a 1.8 nm filter suggest that approximately 80% of the total measurable Pu was in the form of a filterable particulate, in comparison to unfiltered aliquots of the same sample. These results suggest the filterable particles are >1.8 nm but smaller than the 0.2 μm average diameter openings of the Ti porous plate situated at the base of the column. In this advection-dominated system, Pu is migrating principally as or in association with colloids after being released from the LaBS glass. Further analyses using the reaction rate of LaBS glass and the 1-D advection-dispersion equation, suggest that the majority of the Pu that is released will be retained in the region of LaBS glass in a can-in-canister configuration. Also, analyses of reacted LaBS glass particles with SEM-EDS illustrates that Pu may have segregated into a discrete disk-like phase, possibly PuO_2. Separation of the Pu and the neutron absorber Gd during glass dissolution and transport could be a criticality issue for the proposed repository. However, the translation and interpretation of these long-term PUF test results to actual disposed waste packages requires further analysis.

Acknowledgements

The authors express gratitude to Todd Schaef and Steven Baum (both of Pacific Northwest National Laboratory [PNNL]) for their help in analyzing the XRD results discussed in this paper and analyzing the hundreds of solution samples we generated, respectively. Helpful comments provided by D.M. Strachan (PNNL), J.P. Icenhower (PNNL), and two anonymous reviewers are also appreciated. This work was funded by the US Department of Energy under Contract DE-AC06-76RLO 1830. PNNL is

operated for the US Department of Energy by Battelle.

References

Allard, B., Rydberg, J., 1983. Plutonium Chemistry. American Chemical Society.

ASTM, 1994. Standard Test Methods for Determining Chemical Durability of Nuclear Waste Glasses: The Product Consistency Test (PCT). ASTM C1285, American Society for Testing and Materials International, Philadelphia, PA.

ASTM, 2001. Standard Test Methods for Sieve Analysis of Fine and Coarse Aggregates, ASTM C136, American Society for Testing and Materials International, Philadelphia, PA.

Bates, J.K., Bradley, C.R., Buck, E.C., Cunnane, J.C., Ebert, W.L., Feng, X., Mazer, J.J., Wronkiewicz, D.J., Sproull, J., Bourcier, W.L., McGrail, B.P., Altenhofen, M.K., 1994a. High-Level Waste Borosilicate Glass: A Compendium of Corrosion Characteristics, vol. 2, DOE-EM-0177, US Department of Energy Office of Waste Management, Springfield, VA.

Bates, J.K., Bradley, C.R., Buck, E.C., Cunnane, J.C., Ebert, W.L., Feng, X., Mazer, J.J., Wronkiewicz, D.J., Sproull, J., Bourcier, W.L., McGrail, B.P., Altenhofen, M.K., 1994b. High-Level Waste Borosilicate Glass: A Compendium of Corrosion Characteristics, vol. 1, DOE-EM-0177, US Department of Energy Office of Waste Management, Springfield, VA.

Bates, J.K., Ellison, A.J.G., Emery, J.W., Hoh, J.C., 1996. Glass as a waste form for the immobilization of plutonium. In: Murphy, W.M., Knecht, D.A. (Eds.), Proceedings of the Materials Research Society Symposium: Scientific Basis for Nuclear Waste Management XIX, vol 412. Materials Research Society, 57–64.

Bates, J.K., Emery, J.W., Hoh, J.C., Johnson, T.R., 1995. Performance of high plutonium-containing glasses for the immobilization of surplus fissile materials. In: Jain, V., Palmer, R. (Eds.), Environmental Issues and Waste Management Technologies in the Ceramic and Nuclear Industries, vol. 61. American Ceramic Society, Westerville, OH, pp. 47–454.

Bates, J.K., Jardine, L.J., Steindler, M.J., 1982. Hydration aging of nuclear waste glass. Science 218, 51–54.

Bibler, N.E., Ramsey, W.G., Meaker, T.F., Pareizs, J.M., 1996. Durabilities and microstructures of radioactive glasses for immobilization of excess actinides at the Savannah River site. In: Murphy, W.M., Knecht, D.A. (Eds.), Proceedings of the Material Research Symposium: Scientific Basis for Nuclear Waste Management XIX, vol. 412. Materials Research Society, Pittsburgh, PA, 65–72.

Brunauer, S., Emmett, P.H., Teller, E., 1938. Adsorption of gases in multimolecular layers. J. Am. Chem. Soc. 60, 309–319.

Cochran, S.G., Dunlop, W.H., Edmunds, T.A., MacLean, L.M., Gould, T.H., 1997. Fissile Material Disposition Program-Final Immobilization Form Assessment and Recommendation, UCRL-ID-128705, Lawrence Livermore National Laboratory, Livermore, CA.

Conca, J.L.,Wright, J., 1992. Hydrostratigraphy and recharge distribution from direct measurements of hydraulic conductivity using the UFA method. PNL-9424, Pacific Northwest National Laboratory, Richland, WA.

Ebert, W.L., Bates, J.K., 1993. A comparison of glass reaction at high and low glass surface/solution volume. Radioact. Waste Manage. 104, 372–384.

Ebert, W.L., Tam, S.-W., 1997. Dissolution Rates of DWPF Glasses from Long-Term PCT. In: Gray, W.J., Triay, I.R. (Eds), Materials Research Society Symp., Scientific Basis for Nuclear Waste Management XX, vol 465. Materials Research Society, 149–156.

Fortner, J.A., Mertz, C.J., Bakel, A.J., Finch, R.J., Chamberlain, D.B., 2000. Plutonium Silicate Alteration Phases Produced by Aqueous Corrosion of Borosilicate Glass. In: Smith, R.W., Shoesmith, D.W. (Eds)Material Research Symp. Proc. Scientific Basis for Nuclear Waste Management XXIII, vol 608. Materials Research Society, 739–744.

Gamerdinger, A.P., Kaplan, D.I., 2000. Application of a continuous-flow centrifugation method for solute transport in disturbed, unsaturated sediments and illustration of mobile–immobile water. Water Resour. Res. 36, 1747–1755.

Gin, S., Jollivet, P., Mestre, J.P., Jullien, M., Pozo, C., 2001. French SON 68 nuclear glass alteration mechanisms on contact with clay media. Appl. Geochem. 16, 861–881.

Gray, L.W., Kan, T., Shaw, H.F., Armantrout, A., 1997. Plutonium Disposition Via Immobilization in Ceramic or Glass, UCRL-JC-126837, Lawrence Livermore National Laboratory, Livermore, CA.

Jantzen, C.M., Bibler, N.E., 1987. Product consistency test (PCT) for DWPF glass: Part 1, Test development and protocol, DPST-87-575, Savannah River Laboratory, Aiken, SC.

Loffler, J.V., 1932. Chemical Decolorization. Glasstechniche Berichte 10, 204–211.

Marra, J., Ebert, W.L., 2003. Accounting For a Vitrified Plutonium Waste Form in the Yucca Mountain Repository Total System Performance Assessment (TSPA), WSRC-TR-2003-00530, Westinghouse Savannah River Company, Aiken, SC.

McGrail, B.P., Ebert, W.L., Bakel, A.J., Peeler, D.K., 1997b. Measurement of kinetic rate law parameters on a Na–Ca–Al borosilicate glass for low-activity waste. J. Nucl. Mater. 249, 175–189.

McGrail, B.P., Icenhower, J.P., Martin, P.F., Rector, D.R., Schaef, H.T., Rodriguez, E.A., Steele, J.L., 2000b. Low-Activity Waste Glass Studies: FY2000 Summary Report, PNNL-13381, Pacific Northwest National Laboratory, Richland, WA.

McGrail, B.P., Icenhower, J.P., Martin, P.F., Schaef, H.T., O'Hara, M.J., Rodriguez, E.A., Steele, J.L., 2001. Waste Form Release Data Package for the 2001 Immobilized Low-Activity Waste Performance Assessment, PNNL-13043, Rev.2, Pacific Northwest National Laboratory, Richland, WA.

McGrail, B.P., Lindenmeier, C.W., Martin, P.F., 1999. Characterization of Pore Structure and Hydraulic Property Alteration in Pressurized Unsaturated Flow Tests. In: Wronkiewicz, D.J., Lee, J.H. (Eds), Material Research Symp. Proc, Scientific Basis for Nuclear Waste Management, vol. 556. Material Research Society, 421–428.

McGrail, B.P., Lindenmeier, C.W., Martin, P.F., Gee, G.W., 1996. The Pressurized Unsaturated Flow (PUF) Test: A New Method for Engineered-Barrier Materials Evaluation. In: Jain, V., Peeler, D.K. (Eds.), Environmental Issues and Waste Management Technologies in the Ceramic and Nuclear Industries II, vol. 72. The American Ceramic Society, Westerville, Ohio, pp. 17–329.

McGrail, B.P., Martin, P.F., Lindenmeier, C.W., 1997a. Accelerated Testing of Waste Forms Using a Novel Pressurized Unsaturated Flow Method. In: Gray, W.J., Triay, I.R.(Eds), Materials Research Society Symp. Proc. Scientific Basis for Nuclear Waste Management XX, vol 465. Materials Research Society, 253–260.

McGrail, B.P., Martin, P.F., Schaef, H.T., Lindenmeier, C.W., Owen, A.T., 2000a. Glass/Ceramic Interactions. In: Smith, R.W., Shoesmith, D.W. (Eds), The Can-In-Canister Configuration For Disposal Of Excess Weapons Plutonium. Material Research Symp. Proc. Scientific Basis for Nuclear Waste; Management XXIII, vol. 608. Material Research Society, 345–352.

Mertz, C.J., Bakel, A.J., Bates, J.K., Chamberlain, D.B., Fortner, J.A., Hanchar, J.M., Wolf, S.F., 1998. Comparison of the Corrosion Behavior of Plutonium Glasses. In: Peeler, D.K., Marra, J. (Eds.), Environmental Issues and Waste Management Technologies in Ceramic and Nuclear Industries III, vol. 87. American Ceramic Society, Westerville, OH, pp. 11–220.

Myers, B.R., Brummonds, W., Armantrout, G., Shaw, H.F., Jantzen, C.M., Jostsons, A., McKibben, M., Strachan, D.M., Vienna, J.D., 1997. Fissile Materials Disposition Program Technical Evaluation Panel Summary Report: Ceramic and Glass Immobilization Options, UCRL-ID-129315, Lawrence Livermore National Laboratory, Livermore, CA.

Papelis, C., Um, W., Russell, C.E., Chapman, J.B., 2003. Measuring the specific surface area of natural and manmade glasses: effects of formation process, morphology, and particle size. Colloids Surfaces A 215, 221–239.

Pierce, E.M., McGrail, B.P., Rodriguez, E.A., Schaef, H.T., Saripalli, K.P., Serne, R.J., Krupka, K.M., Martin, P.F., Baum, S.R., Geiszler, K.N., Reed, L.R., Shaw, W.J., 2004. Waste Form Release Data Package for the 2005 Integrated Disposal Facility Performance Assessment, PNNL-14805, Pacific Northwest National Laboratory, Richland, WA.

Pierce, E.M., McGrail, B.P., Valenta, M.M., Strachan, D.M., 2006. The accelerated weathering of a radioactive low-activity waste glass under hydraulically unsaturated conditions: experimental results from a pressurized unsaturated flow (PUF) test. Nucl. Technol. 155, 133–148.

Plodinec, M.J., 1979. Development of Glass Compositions for Immobilization of SRP Waste, DP-1517. Savannah River Laboratory, Aiken, South Carolina.

Rai, D., Bolton, H., Moore, D.A., Hess, N.J., Choppin, G.R., 2001. Thermodynamic model for the solubility of PuO_2 (am) in the aqueous Na^+–H^+–OH^-–Cl^-–H_2O–ethylenediaminetetracetate system. Radiochim. Acta 89, 67–74.

Rai, D., Hess, N.J., Felmy, A.R., Moore, D.A., Yui, M., Vitorge, P., 1999. A Thermodynamic Model for the Solubility of PuO_2 (am) in the aqueous K^+–HCO_3^-–CO_3^{2-}–OH^-–H_2O System. Radiochim. Acta 86, 89–99.

Ramsey, W.G., Bibler, N.E., Meaker, T.F., 1995. Compositions and durabilities of glasses for immobilization of plutonium and uranium. In: Symposium of Waste Management, University of Arizona, Waste Management Symposia, Inc., 23828–23907.

Rankin, D.T., Gould, T.H., 2000. Plutonium immobilization program: can-in-canister. In: Chandler, G.T., Feng, X. (Eds.), Environmental Issues and Waste Management Technologies in the Ceramic and Nuclear Industries V, vol. 107. The American Ceramic Society, Westerville, OH, pp. 95–500.

Strachan, D.M., Schaef, H.T., Schweiger, M.J., Simmons, K.L., Woodcock, L.J., 2003. A versatile and inexpensive XRD specimen holder for highly radioactive or hazardous specimens. Powder Diffr. 18, 23–28.

Strachan, D.M., Bakel, A.J., Buck, E.C., Chamberlain, D.B., Fortner, J.A., Mertz, C.J., Wolf, S.F., Bourcier, W.L., Ebbinghaus, B.B., Shaw, H.F., Van Konynenburg, R.A., McGrail, B.P., Vienna, J.D., Marra, J., Peeler, D.K., 1998. The characterization and testing of candidate immobilization forms for the disposal of plutonium. In: Symposium of Waste Management 1998, University of Arizona, Waste Management Symposia, Inc.

van Genuchten, M.T., Alves, W.J., 1982. Analytical Solutions of the One-Dimensional Convection-Dispersive Solute Transport Equation, 1661, United States Department of Agriculture.

Vernaz, E., Gin, S., Jegou, C., Ribet, I., 2001. Present understanding of R7T7 glass alteration kinetics and their impact on long-term behavior modeling. J. Nucl. Mater. 298, 27–36.

Vienna, J.D., Alexander, D.L., Li, H., Schweiger, M.J., Peeler, D.K., Meaker, T.F., 1996. Plutonium Dioxide Dissolution in Glass, PNNL-11346, UC-510, Pacific Northwest National Laboratory, Richland, WA.

Wierenga, P.J., Young, M.H., Gee, G.W., Hills, R.G., Kincaid, C.T., Nicholson, T.J., Cady, R.E., 1993. Soil Characterization Methods for Unsaturated Low-Level Waste Sites, PNL-8480, Pacific Northwest Laboratory, Richland, Washington.

Wolery, T.J., 1992. EQ3NR, A Computer Program for Geochemical Aqueous Speciation-Solubility Calculations: Theoretical Manual, User's Guide, and Related Documentation (Version 7.0), UCRL-MA-110662 PT III, Lawrence Livermore National Laboratory, Livermore, CA.

Wolff-Boenisch, D., Gislason, S.R., Oelkers, E.H., Putnis, C., 2004. The dissolution rates of natural glasses as a function of their composition at pH 4 and 10.6, and temperatures from 25 to 74 °C. Geochim. Cosmochim. Acta 68, 4843–4858.